Removal of metals from aqueous solutions using dried Cladophora parriaudii of varying biochemical composition

Ross, Michael; Stanley, Michele; Day, John; Semiao, Andrea JC

Published in:
Journal of Environmental Management

Publication date:
2021

Removal of metals from aqueous solutions using dried *Cladophora parriaudii* of varying biochemical composition

Michael E. Ross [a*], Michele S. Stanley [a], John G. Day [a], Andrea J.C. Semião [b]

[a] Scottish Association for Marine Science (SAMS), Scottish Marine Institute, Oban, Argyll, PA37 1QA, UK

[b] School of Engineering, The University of Edinburgh, Edinburgh, EH9 3FB, UK

corresponding author*: michael.ross@sams.ac.uk

Michele.stanley@sams.ac.uk

John.day@sams.ac.uk

Andrea.semiao@ed.ac.uk

Abstract

Macroalgal biosorption has shown promise for the removal of metal ions from wastewaters, whose presence can pose a threat to the aquatic environment. There is a wealth of literature published on macroalgal biosorption, the common thread being that the biosorbent material was collected from the field, under undefined conditions. These studies offer little insight into the impact of prior cultivation or biomass production practices upon the biosorbent material, its adsorptive physico-chemical properties and its subsequent capacity for metal removal. The present study sought to investigate the influence of changes in macroalgal cultivation, specifically nutrient regime, upon biomass properties and the resultant adsorption performance. The macroalga *Cladophora parriaudii* was cultivated under six different nutrient regimes; 2:1 and 12:1 N:P molar ratios, with nitrogen supplied either as ammonium (NH_4^+), nitrate (NO_3^-), or urea ($CO(NH_2)_2$). These nutrient regimes were designed to produce biomass of varying biochemical and cell surface profiles. After cultivation, the biomass was rinsed, dried, biochemically analysed and then used for the removal of four individual metals from solution. Metal removal varied considerably between treatments and across initial metal concentrations, with removal values of 46-85%, 9-80%, 8-71%, and 49-94% achieved for Al, Cu, Mn, and Pb, respectively, with initial metal concentrations varying between 0-150 mg L^{-1}. The observed variation in metal removal can only be attributed to differences in biochemistry and cell surface properties of the biosorbent induced by nutrient regime, as all other variables were constant. This study demonstrates that prior cultivation conditions influence the biochemistry of a biosorbent material, namely macroalgae *Cladophora parriaudii,* which has an impact upon metal removal. This aspect should be given due consideration for future biosorption research and when reviewing already published literature.

Keywords:

Cladophora; Heavy metals; Biochemical composition; Adsorption; Copper; Macroalgae

Highlights:

- Algal biomass composition varied with nutrient regime.
- Metal containing clusters appeared on the cell surface following metal exposure.
- Biomass of varying composition resulted in differing metal adsorption performance.
- More copper was removed from solution when biomass was rich in carbohydrates.

1. Introduction

A global growing population and consequential industrial growth has led to the contamination of numerous water bodies with toxic or heavy metals (Kotrba, 2011; Wang and Chen, 2009). Concentrations of copper and lead in surface waters have been reported to be in excess of the WHOs recommended drinking-water guidelines (Table 1).

Table 1. Concentrations of copper and lead found in surface waters and their permissible limits in drinking water according to the WHO guidelines.

Water Type	Copper		Lead		References
	(mg L^{-1})	(mmol L^{-1})	(mg L^{-1})	(mmol L^{-1})	
Surface Waters	0.002 – 3.95	$3.2 * 10^{-5}$ – $6.2 * 10^{-2}$	0.0003 - 0.4	$1.5 * 10^{-6}$ – $1.9 * 10^{-3}$	(Kar et al., 2008; Reza and Singh, 2010; Varol and Şen, 2012)
Drinking Water Quality	1	$3.15 * 10^{-2}$	0.01	$4.8 * 10^{-5}$	(WHO, 2017)

The presence of toxic or heavy metals in water is a pertinent global problem (Ali et al., 2013; He and Chen, 2014; Islam et al., 2015), therefore, the removal of heavy or toxic metals from wastewaters is of paramount importance to preserve human, aquatic, and environmental health. Conventional treatment technologies, including membrane technology, ion exchange, and activated carbon have disadvantages, such as high capital and/or operational costs, as well as toxic sludge generation (Fulazzaky et al., 2019, 2015; Sepehri et al., 2020). Metal ion removal efficiency can be low for reverse osmosis (85%) and ion exchange (55%) technologies, especially when treating large volumes of wastewater containing a low concentration of metal ions (Fu and Wang, 2011; Pap et al., 2020; Zhang et al., 2009). This is of particular importance for wastewater polishing or wastewater tertiary treatment since some metals are toxic even at low concentrations (Tchounwou et al., 2012). Furthermore, ion exchange resins have to undergo chemical regeneration once they are "exhausted", which leads to the development of secondary waste streams (Fu and Wang, 2011).

Therefore, novel and sustainable processes for the removal of toxic elements from solution should be sought. An alternative for metal removal from wastewaters is biosorption (Mack et al., 2007; Utomo et al., 2016; Volesky and Holan, 1995), *i.e.* the sorption of metals using material of a biological origin, which encompasses both absorption and adsorption (Gadd, 2009). Macro-algae, in particular, are viewed as promising candidates for biosorption purposes, given their general ubiquity, abundance and high metal sorption capacity (Figueira et al., 2016; Henriques et al., 2017). Considerations into species selection, standardisation of biomass collection *vs* biomass production, suitability of different wastewater streams, removal of co-existing contaminants, recovery of metals/contaminants, circularity/reusability of the biosorbent material following pollutant removal, process implementation and scalability, and techno-economic and environmental life cycle assessments need to be researched.

There are a variety of biotic and abiotic factors which influence biosorption including pH, temperature, initial metal concentration and the presence of co-existing ions (Mehta and Gaur, 2005; Özer et al., 2004). In addition, the properties of the biosorbent material will also affect metal sorption, including the species, whether it is living or not, its surface area, initial biosorbent dosage, and any pre-treatment of biomass *e.g.* immobilization or chemical modification (Camacho et al., 2013; Chojnacka et al., 2004; Figueira et al., 2016; Gadd, 2000; Özer et al., 2004; Tien, 2002). Moreover, the type and abundance of functional groups of the species studied will also have an impact upon both the type of metals/contaminants removed and overall sorption capacity (Figueira et al., 2016). It is known that differences in macro-algal culture conditions will elicit a change in the biochemical content of its biomass (Ross et al., 2018). For instance, Schiener et al., (2015) reported that across a 14 month time-frame, the tissue C and N % of wild populations of *Saccharina latissima* ranged from 21.1-30.5% and 0.8-2.2%, respectively. Therefore, differences in cultivation conditions (including nutrient regime) will influence the biochemical composition of the biomass and may result in an alteration in the quantity and quality of functional groups present on the cell surface; this in turn, may have a resultant impact upon its metal removal capacity. There is a wealth of literature

pertaining to metal removal with macro-algal biomass with recent results reporting removal values of 50-70%, 55-80%, and 5-97.5% for cadmium, lead, and nickel, respectively; this highlights the potential that macroalgal biomass has as a biosorbent for recalcitrant pollutants (Amro and Abhary, 2019; Arumugam et al., 2020; El-Naggar and Rabei, 2020). However, minimal attention has been paid to the impact of algal cultivation conditions and/or biomass production on the resultant metal biosorption. Instead, the majority of studies focus upon the optimisation of process parameters (e.g. pH) utilising biological material of a given species that has been collected from the field (Amro and Abhary, 2019; Arumugam et al., 2020; El-Naggar and Rabei, 2020; Topal et al., 2020; Zhang et al., 2019). The drawback of these studies is that they do not provide any background information relating to the life or nutritional history of the biomass, the environmental conditions in which it was produced, age, time spent washed ashore, if it exhibits any signs of bacterial degradation or presence of epiphytes, or if it has been previously exposed to contaminants during its growth, including heavy metals. Essentially, the studies employ a biomass of unknown biochemical composition, propagated under undefined conditions for metal removal optimisation. From a wastewater treatment perspective, there is a demand for a low-cost material which can be produced in bulk and of consistent quality for contaminant removal purposes (Calderón et al., 2020; Pap et al., 2020). Previously published macroalgal biosorption studies may indicate material of a given type, collected at a given time, with potential bioremediation promise, however, they may be of negligible practical significance since there is no information provided regarding the biomass production.

The main aim of this study was to investigate the influence of macroalgal production practices, specifically nutrient regime, upon the quality of harvested biomass and the impact that this has upon metal removal. To test this hypothesis, *Cladophora parriaudii* was cultivated with three different nitrogen sources: ammonium (NH_4^+) nitrate (NO_3^-) and urea, and at two different N:P ratios (2:1 and 12:1) known to produce biomass with differing bulk chemical compositions (Ross et al., 2018). The filamentous macro-alga *C. parriaudii* was selected as a model organism due to its large surface area, ubiquity, abundance, and ease of harvest making it a strong candidate species for metal removal

applications (Ross et al., 2017). To simplify the sorption process, the biomass produced was dried and then used for the adsorption of four different heavy or toxic metals, namely Al, Cu, Mn and Pb. These metals were selected based upon their prevalence in the environment, varying degrees of toxicity (low-high), and whether or not they have any known function within an algal cell and hence may have some uptake mechanism in place (Förstner and Wittmann, 1981; Raven et al., 1999). The experimental conditions used in this study were selected based upon optimal values obtained from an in-depth literature review (Davis et al., 2000; Lee and Chang, 2011; Prasher et al., 2004). Characterisation of biomass and metal removal analyses was conducted using a suite of biochemical and analytical methods including inductively coupled plasma optical emission spectrometry (ICP-OES), Fourier transform infrared spectroscopy (FTIR), and scanning electron microscopy with energy dispersive X-ray analysis (SEM-EDX).

2. Materials and Methods

2.1. Algal cultivation

The green filamentous macro-alga *Cladophora parriaudii* CCAP 505/09 was obtained from the Culture Collection of Algae and Protozoa (CCAP), at the Scottish Association for Marine Science (SAMS, UK). Algal biomass was incubated in an illuminated shaker (Sartorius Stedim Biotech, Germany) at 100 rpm at 24°C, under an 18:6 h L:D (Light:Dark) photoperiod, with 30-40 µmol photons m^{-2} s^{-1} of photosynthetically active radiation (PAR: 400-700). Algae were grown in six variations of modified Guillard's f/2 medium (Guillard and Ryther, 1962), based on artificial seawater at 33.5 g L^{-1} (Instant Ocean, UK) (Ross et al., 2018). Nitrogen (N) and phosphorous (P) were supplied as either ammonium (NH_4^+), nitrate (NO_3^-), or urea ($CO(NH_2)_2$) at 2:1 or 12:1 N:P molar ratios, corresponding to an initial N content of 160 or 960 µM, respectively. Algal sub-cultures were pre-acclimated in experimental media and conditions for 7 days prior to the commencement of growth.

Triplicate 1 L flasks containing 650 mL of media were inoculated with 465 mg fresh weight *C. parriaudii* and maintained under the conditions described above. After 14 days, all cultures were harvested, rinsed with deionised water to remove extracellular salts and nutrients. Residual water was removed using a reticulated spinner (Ross et al., 2017). Harvested biomass was frozen and lyophilised overnight (Modulyo 4K Freeze-Dryer, Edwards, UK). This freeze-dried biomass was used as the feedstock for biosorption trials, as well as for biochemical analysis.

2.2. Biochemical analyses

Protein was extracted using hot-trichloroacetic acid and overnight incubation in an alkaline solution before quantification using the Lowry assay (Slocombe et al., 2013). Total soluble carbohydrate content of the biomass was assessed using a modified phenol-sulphuric acid method (Fournier, 2001) , originally described by (Dubois et al., 1956). Briefly, 2.5 mL of 1M H_2SO_4 is added to 5 mg of dry weight (DW) biomass and acid-hydrolysed in an autoclave at 121°C for 15 min at 1.14 bar (TCR/40/H, Touchclave-R, LTE Scientific, UK). Once cooled to room temperature (RT = ~20-25°C), 30 µL of the hydrolysate was reacted with 0.5 mL of 4% phenol (*w/v*) followed by the direct addition of 2.5 mL of concentrated H_2SO_4. Once cooled to RT, the mixture was read in a spectrophotometer at 490 nm (Heλios Gamma UV-vis spectrophotometer, Thermo Scientific, UK). Pigments were extracted from biomass using a method based on (Griffiths et al., 2011), where 2 mL of dimethylsulfoxide (DMSO) was added to 1.5 mg of biomass and incubated overnight in a dark water bath at 60°C. The ash content of the biomass followed a standard method (Sluiter et al., 2008). The biochemical components were all expressed as a % DW, with any of the biomass that was unaccounted for described as “other”.

2.3. Stock and feed solutions

193 Heavy metal stock solutions (1000 mg L^{-1}) were prepared by dissolving $Al_2(SO_4)\cdot 16H_2O$, $CuSO_4\cdot 5H_2O$,
194 $MnCl_2\cdot 4H_2O$ or $PbCl_2$ in ultrapure water (18.2 MΩ.cm^{-1}), with a few drops of HNO_3 (Aristar® grade,
195 VWR, UK) added to avoid metal precipitation. All powdered chemicals were obtained from Fisher
196 Scientific (UK) and were of analytical grade (95-99%). Working metal concentrations of 1, 10, 40, 80,
197 and 150 mg L^{-1} were created by diluting with deionised water. This concentration range was selected
198 in order to determine the maximum sorption capacity of the biomass, rather than mimicking what is
199 experienced in the environment. The pH was adjusted to 4.5 using either 0.1 M HCl or NaOH (Davis
200 et al., 2000).
201

202 2.4. Metal sorption protocol

203 Metal sorption experiments were performed in multi-well plates housed in an incubated shaker
204 (Sartorius Stedim Biotech, Germany) at 100 rpm, 24°C, and at atmospheric pressure, with a non-
205 living biosorbent dose of 1 g L^{-1} (Lee and Chang, 2011). Experiments were incubated for 24 h to allow
206 sufficient time for metal sorption equilibrium (Prasher et al., 2004). Algal material was then removed
207 from the individual wells and placed in individual micro-centrifuge tubes and dried overnight in an
208 oven at 60°C. The remaining metal solutions were transferred to individual centrifuge tubes and
209 acidified with a few drops of HNO_3 (Aristar® grade, VWR, UK) to prevent precipitation and
210 subsequently analysed for metal concentration.
211

212 2.5. Multi-elemental analysis

213 Metal solutions were analysed by ICP-OES (Optima 5300 DV, Perkin Elmer, UK) at the School of
214 Chemistry, University of Edinburgh (Darmovzalova et al., 2020). The ICP-OES utilised a radio
215 frequency forward power of 1400 W, with Ar gas flows of 15, 0.2, and 0.75 L min^{-1} for plasma,
216 auxiliary, and nebuliser, respectively. A peristaltic pump was employed to draw the sample into a

Gem Tip Cross-Flow Nebuliser and Scott's Spray Chamber at 1.5 mL min^{-1}. In all instances, the instrument was operated in axial mode. On each sampling occasion, calibration standards were prepared for each metal using single element 1000 mg L^{-1} standards (Fisher Scientific, UK), diluted with 2% HNO_3 (*v/v*) (Aristar® grade, VWR, UK). Several wavelengths were initially selected for each element and were analysed in a fully quantifiable mode (three points per unit wavelength), with three replicates employed per sample. A single wavelength for each element was selected for reporting results based upon the peak shape, background interference, sensitivity, and the linearity of the calibration curve. The selected wavelengths were 308.213 nm, 324.752 nm, 259.372 nm, and 220.353 nm for Al, Cu, Mn, and Pb, respectively. All calibration curves had a linear regression of $R^2 \geq$ 0.99993. Blanks and internal standards were analysed periodically to ensure the accuracy of the method.

2.6. FT-IR analysis

FT-IR spectroscopy was used to detect vibrational frequency changes in algal biomass before and after metal sorption. Spectra were collected using FT-IR attenuated total reflectance (ATR) using a Perkin Elmer (UK) Frontier at the Institute for Materials and Processes, School of Engineering, University of Edinburgh. The FT-IR is equipped with a diamond crystal Universal ATR Sampling Accessory and with a mercury cadmium telluride detector. Samples were scanned over a wavenumber range of 4000 - 650 cm^{-1} at a resolution of 2 cm^{-1}. Approximately 1-2 mg of lyophilised biomass was placed onto the crystal surface and pressed into the crystal head at a force of 60 arbitrary units. Each sample consisted of an average of 25 scans. Sample scans were recorded using Spectrum software (v. 10, Perkin Elmer), with the background automatically corrected for air and atmospheric CO_2/H_2O.

2.7. SEM analysis

After biosorption, dried algal biomass was mounted onto specimen stubs and coated in carbon (BTT-IV carbon evaporation coater, Denton Vacuum, USA). Samples were visualised using a scanning electron microscope (Zeiss SIGMA HD VP FE-SEM, Carl Zeiss Microscopy, UK) at the School of GeoSciences, University of Edinburgh (Manning et al., 2017). Images were recorded using the back-scattered electrons technique (BSE). SEM energy-dispersive X-ray (EDX) analysis (Aztec EDS system, Oxford Instruments) was performed on samples utilising an accelerating voltage of 20 kV, an aperture size of 30 µm, and a working distance of 7 ± 1 mm.

2.8. Metal removal

Metal sorption is primarily presented as the metal removal per unit dry weight biomass (mmol g^{-1} DW) at each initial metal concentration (C0). The percentage of metal removal and variance in removal is also presented. To ease comparison with literature, Langmuir and Freundlich equilibrium adsorption isotherms were modelled, and the data presented in the supplementary material.
The capacity of sorption by *C. parriaudii* biomass is characterised by the mass balance Equation (1):

$$Qe\ (mmol\ g^{-1}) = \frac{V(C0 - Ce)}{S} \quad (1)$$

Where, *Qe* is the metal sorbed at equilibrium (mmol g^{-1}), *V* is the volume of solution (L), *C*0 and *Ce* are the initial and final (equilibrium) concentrations in solution (mmol L^{-1}), respectively, and *S* is the biosorbent dose (g). Equilibrium sorption isotherms, used to describe the relationship between the concentration of sorbed metal and metal in solution at a given temperature, were generated by plotting *Qe* against *Ce*. The Langmuir and Freundlich models were then used to characterise biosorption. The Langmuir adsorption isotherm is described using Equation (2) (Gadd, 2009; Langmuir, 1918):

$$Qe\ (mmol\ g^{-1}) = \frac{Qmax \cdot b \cdot Ce}{1 + b \cdot Ce} \quad (2)$$

Where *Qmax* is the maximum adsorption capacity by the biosorbent per unit mass, *b* is an affinity parameter related to the energy of adsorption and indicates the strength of attraction of the sorbent for the solute (Deng et al., 2007).

The Freundlich isotherm is described using Equation (3) (Freundlich, 1907; Gadd, 2009):

$$Qe\ (mmol\ g^{-1}) = K_F \cdot Ce^{\frac{1}{n}} \quad (3)$$

Where K_F and *n* are Freundlich constants and respectively relate to the adsorption capacity and adsorption intensity of the biosorbent (Deng et al., 2007). Coefficients used to describe biosorption were obtained by first linearizing equations 2 and 3.

2.9. Data analysis

All experiments were performed in triplicate, unless otherwise stated, and the experimental error was calculated and expressed as one standard deviation (SD). Data regarding the biochemical composition of the biomass is portrayed as a proportion of its dry weight (% DW). A one-way ANOVA with Tukey's post hoc analysis was used to determine significant differences in the biochemical composition of the biomass. Levels of significance were set at $p < 0.05$. All statistical analyses were performed using Minitab® Statistical Software version 17.

3. Results and Discussion

In order to understand the influence of the nutritional history on macro-algal cellular characteristics and biosorbent metal capacity, *Cladophora parriaudii* was cultivated under different nutrient regimes as described in a previous study by many of the same authors (Ross et al., 2018). After the

293 cultivation period, algal samples were harvested, dried, and biochemically characterised. Following
294 this, four different types of metals across a concentration range, were independently adsorbed onto
295 the dried biomass. Metals, namely Al, Cu, Mn and Pb, were selected based upon their environmental
296 prevalence, toxicological effect, and biological role within an algal cell.

297 3.1. Biochemical Composition

298 The main aim of this research was to investigate the effect that the nutritional history has on algal
299 biomass composition and how this then influences its capacity for metal removal. *C. parriaudii* was
300 cultivated under six different nutrient regimes, designed to produce biological material of varying
301 chemical composition: these were formulated using three different N sources (NH_4^+, NO_3^-, and urea)
302 supplied at two N:P ratios (2:1 and 12:1). As previously found by the authors, (Ross et al., 2018), the
303 selected nutrient regimes, in particular the nitrogen type and N:P ratio, exerted a great influence
304 upon the final biochemical composition of *C. parriaudii* biomass, with results shown in Table 2. For
305 instance, biomass cultivated under a 2:1 N:P regime had a greater carbohydrate (39.6-44.2% DW)
306 and lower protein content (8.5-10.5% DW) in comparison to that maintained under a 12:1 regime,
307 with values ranging from 32-37.5% DW and 11.5%-13.6% DW, respectively. Biomass cultivated under
308 a 12:1 NO_3^- regime had a greater carbohydrate and lower protein yield than its molar equivalent
309 cultivated with either NH_4^+ or urea, thus making it more akin to biomass cultivated with 2:1 N:P
310 conditions. The differences in carbohydrate and protein are statistically significant when either NH_4^+
311 or urea were employed as the N source (p = 0.005-0.015). These nitrogen forms may be removed
312 favourably from the growth medium due to either their lower energetic requirement for assimilation
313 or via the provision of a supplementary carbon source (Ross et al., 2018). The uptake of these N
314 forms would likely have been enhanced, resulting in an extended duration of N-limitation under the
315 2:1 regime, or greater N removal from the 12:1 regime. This will have an influence on the
316 biochemical composition. For instance, macro-algae have been found to synthesise proteins and

chlorophylls under N sufficiency, with a shift towards the accumulation of storage polysaccharides when nitrogen deprived (Chopin et al., 1995).

Biomass grown in 12:1 N:P regimes had a marginally higher pigment content (0.9-1.1% DW) in comparison to the 2:1 ratios (0.7-1.1% DW). The ash content of *C. parriaudii* cultivated under a 2:1 NO_3^- regime was greater (36.7% DW) than all others which were in the range of 29.4-33.5% DW (Table 2): however, this was not statistically significant ($n = 1$). The remaining component of the biomass has been pooled and defined as "other" (Table 2) and will most likely comprise of incomplete extractions or non-soluble macromolecules, lipids, uronic acids, secondary metabolites, free amino acids, nucleic acids, and other organic material. These results indicate that the nutrient regime has a strong influence upon the final composition of *C. parriuadii*. However, this data alone is insufficient to ascertain if there are differences in cell surface properties and what effect this may have on metal adsorption.

Table 2. The biochemical composition of the dry weight (DW) *Cladophora parriaudii* cultivated under different nutrient regimes. Biochemical components that are denoted by different letters are statistically significant ($p < 0.05$).

Biochemical Component (% DW)	NH_4^+		NO_3^-		Urea	
	2:1	**12:1**	**2:1**	**12:1**	**2:1**	**12:1**
Ash	33.5	29.4	36.7	31.4	31.8	32.0
Carbohydrate	44.2^{a}	34.0^{bc}	39.6^{abc}	37.5^{abc}	41.0^{ab}	32.0^{c}
Pigments	0.8^{a}	1.1^{a}	1.1^{a}	0.9^{a}	0.7^{a}	1.0^{a}
Protein	8.5^{b}	13.3^{a}	10.5^{ab}	11.5^{ab}	9.5^{ab}	13.6^{a}
Other	13.1^{bc}	22.1^{a}	12.3^{c}	18.6^{abc}	17.0^{abc}	21.3^{ab}

3.2. Metal Removal

Experiments were performed in order to determine whether there was a difference in metal removal performance by non-living *C. parriaudii* biomass after cultivation under six different nutrient regimes. To test the removal capacity of Al, Cu, Mn, and Pb, were independently tested across a

range of working concentrations (1-150 mg L^{-1}). In this study, sorption is principally presented as the concentration of metal sorbed per unit of dried biomass (mmol g^{-1}) and as a proportion of metals removed from solution (Figs 1-4), as described in section 2.8. For the purpose of comparison with literature, Langmuir and Freundlich adsorption isotherms were modelled as well, with isotherm parameters shown in (Supplementary Information Table S1). These models have their deficiencies when used to describe adsorption using a biological material. For instance, the Langmuir model assumes that sorption occurs as a monolayer, while Freundlich assumes a constant pH which is very unlikely in an unbuffered system where ion exchange will result in H^+ displacement by binding cations (Gadd, 2009; Mehta and Gaur, 2005).

There was a broad variation in the biosorption capacity between both metals and nutrient regimes. Metal removal per unit biomass ranged from 0.023-1.636 (Q_{max} = 1.08-2.35), 0.005-0.885 (Q_{max} = 0.3-0.62), 0.005-0.658 (Q_{max} = 0.22-0.48), and 0.002-0.855 (Q_{max} = 0.43-0.61) mmol g^{-1} DW for Al, Cu, Mn, and Pb, respectively (Figs 1-4 & Supplementary Table S1). These equate to 45.7-82.5%, 9.2-79.9%, 8.2-71.3%, and 48.8-93.7% removal of the initial metal concentration (C0), respectively. These results are comparable to maximum removal values (Q_{max}) for single metal solutions recorded elsewhere with other macroalgal biosorbents: of 2.79-2.865 (Lee et al., 2004; Sari and Tuzen, 2009) , 0.266-1.61 (Deng et al., 2006; Romera et al., 2007) , 0.7–1.07 (Henriques et al., 2011; Vijayaraghavan and Joshi, 2014), and 0.139-1.815 (Holan and Volesky, 1994; Pavasant et al., 2006) mmol g^{-1} DW for Al, Cu, Mn, and Pb, respectively. While the values obtained within this study are generally within range of those reported elsewhere, direct comparison with these studies may be unfair. Most of these studies focussed upon the optimisation of process parameters (e.g. pH, temperature) with their given material to maximise metal removal, while this approach was not undertaken within this study. As a result, the metal removal values presented in this study may be an underestimation of the theoretical maximum. Furthermore, a common feature of all the above cited literature is that they all employ biomass collected from the field and do not provide any

background information relating to its propagation. Whilst some of the recorded values are high and show promise for metal removal purposes, the removal values were obtained with a biomass collected at a very particular time under undefined environmental conditions. Therefore, producing a biomass with the same qualities for scientific reproducibility or practical application, such as wastewater treatment, would be challenging. The importance of knowledge underpinning biomass production is demonstrated within this study, as variation in metal sorption between treatments can only be attributed to differences in the biochemical and structural composition of the *Cladophora* biomass, elicited by variability in nutrient regime provided, since all other experimental process factors were constant.

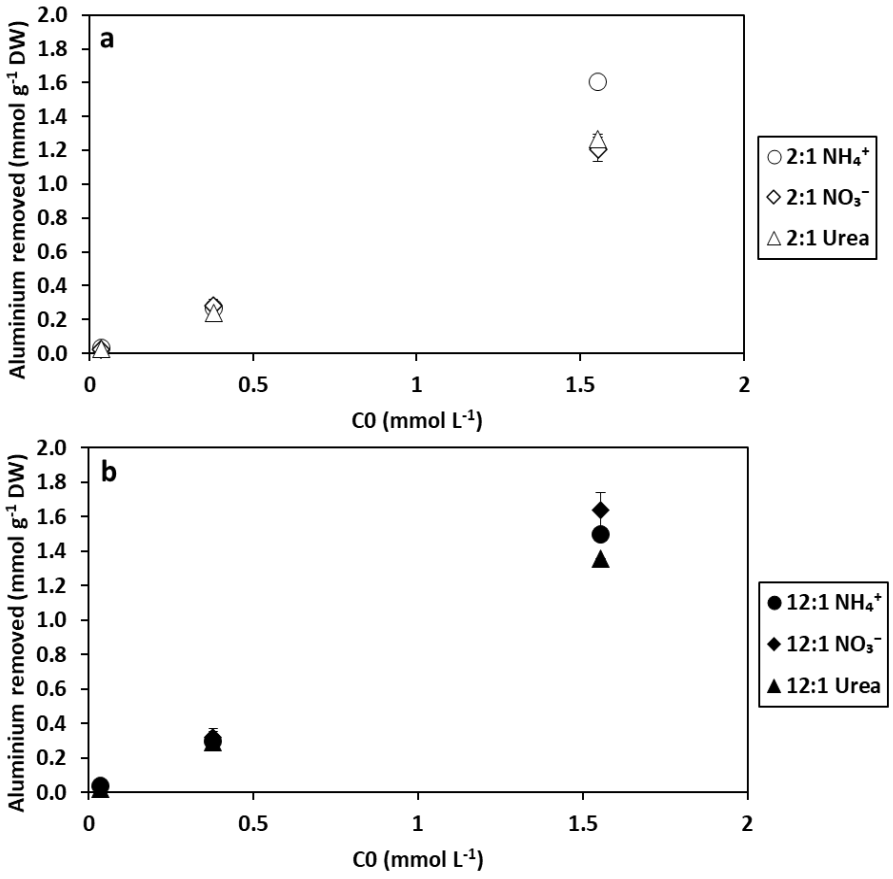

Figure 1. Aluminium removal per unit dry weight (DW) by *Cladophora parriaudii* biomass previously cultivated under different N:P ratios and nitrogen types; (**a**) 2:1 NH_4^+ (white circle), 2:1 NO_3^- (white diamond), 2:1 urea (white triangle), (**b**) 12:1 NH_4^+ (black circle) 12:1 NO_3^- (black diamond), 12:1 urea (black triangle). The sorption conditions were; pH = 4.5, contact time = 24 h, biosorbent dose = 1 g L^-

376 ^{1}, agitation = 100 rpm, initial metal concentration (C0) = 0.035-1.55 mmol L^{-1}, temperature = 24°C,
377 light = constant with 30-40 µmol photons m^{-2} s^{-1} (*n* = 1-3, *error bars* = 1 SD).

378

379 Removal of aluminium and lead followed an almost linear trend, albeit with a slight plateau
380 occurring with lead, with similarity in metal removal at all initial metal concentrations, and
381 irrespective of the nutrient regime in which the biomass was previously cultivated under (Figs. 1 &
382 2). This was coupled with very low levels of variance for both Al (<0.0304) and Pb (<0.0096). Neither
383 aluminium nor lead serve any known function within the algal cell, therefore, it could be postulated
384 that metal bonding may be indiscriminate with no preference exhibited for certain types of
385 functional groups or specific uptake channels. Results reported elsewhere verify this, by
386 demonstrating that a multitude of different functional groups are involved in the adsorption of
387 aluminium and lead, including amide, carbonyl, carboxyl, hydroxyl, and sulfonate (Amro and Abhary,
388 2019; Sari and Tuzen, 2009). This suggests that the biological influence may play a lesser role with
389 non-essential metals.

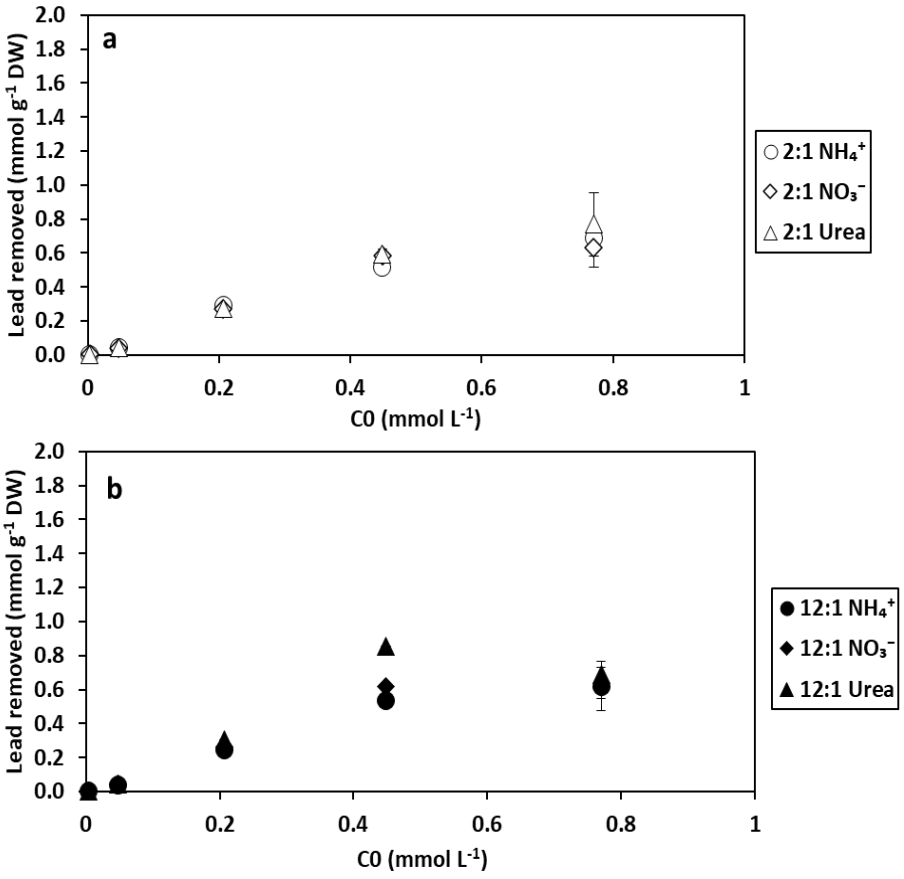

390

391 **Figure 2.** Lead removal per unit dry weight (DW) by *Cladophora parriaudii* biomass previously
392 cultivated under different N:P ratios and nitrogen types; (**a**) 2:1 NH_4^+ (white circle), 2:1 NO_3^- (white
393 diamond), 2:1 urea (white triangle), (**b**) 12:1 NH_4^+ (black circle) 12:1 NO_3^- (black diamond), 12:1 urea
394 (black triangle). The sorption conditions were; pH = 4.5, contact time = 24 h, biosorbent dose = 1 g L^{-1},
395 agitation = 100 rpm, initial metal concentration (C0) = 0.004-0.78 mmol L^{-1}, temperature = 24°C,
396 light = constant with 30-40 µmol photons m^{-2} s^{-1} (*n* = 1-3, *error bars* = 1 SD).

397

398 On the other hand, copper and manganese removal followed a linear trend until reaching a more
399 pronounced plateau (Figs 3 & 4), suggesting that the biosorbent material reached its metal
400 adsorption saturation capacity upon exposure to 40-80 mg L^{-1}. This is somewhat earlier than what
401 was observed with aluminium and lead (Figs 1 & 2). There are several putative reasons for this.
402 Firstly, Cu and Mn are trace metals that are essential for algal growth, being involved in electron
403 transport and oxygen evolution during photosynthesis (Blaby-Haas and Merchant, 2012; Sauer,
404 1980). These metals may preferentially bind to specific sites on the cell surface, for instance channel

transporters or phytochelatins (Navarrete et al., 2019). Secondly, the *C. parriaudii* biomass was previously cultivated in f/2 medium which contains trace concentrations of Cu and Mn (Guillard and Ryther, 1962). Therefore, despite rinsing with deionised water after cultivation, the biomass would have contained these metals both intra- and extra-cellularly. This will likely have resulted in an underestimation of the capacity for the biomass to remove these metals. In comparison to Al and Pb, there was greater variability in metal removal both between nitrogen type and N:P ratio for these essential metals. However, low variability was observed in Mn removal when the biosorbent had been cultivated under a 12:1 N:P ratio (Fig. 3b), which translated to a more protein-rich biomass (Table 2). The inverse is true of copper (Fig. 4), where the greatest removal coupled with low variability in metal removal occurred when the biomass had been previously cultivated under a 2:1 N:P regime or with 12:1 NO_3^-. These biomass types have greater yields of carbohydrates (37.5-44.2% DW) compared to those cultivated with 12:1 N:P with NH_4^+ or urea as the N source (<34% DW) (Table 2). This suggests that copper may be more strongly attracted to functional groups associated with cell wall and membrane mono- and poly-saccharides. Functional groups associated with these structural carbohydrates (e.g. hydroxyl and carboxyl) have been reported to be involved in metal removal by the green macro-alga *Codium vermilara* (Fawzy, 2020).

These results illustrate the influence that biochemistry and methods for producing biomaterial used in biosorption research has and may explain the broad variation in results reported in literature, especially since there is a paucity of information relating the production of the material used in this scientific discipline. However, to more fully understand this, more analyses of the cellular properties is required.

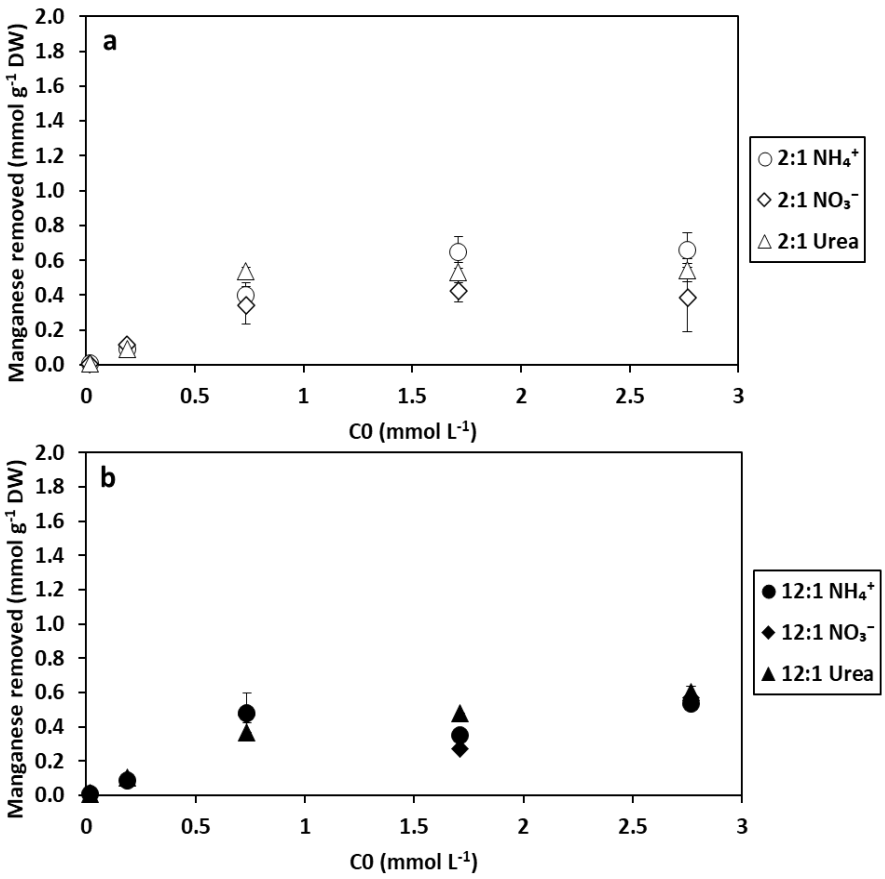

427

428 **Figure 3.** Manganese removal per unit dry weight (DW) by *Cladophora parriaudii* biomass previously
429 cultivated under different N:P ratios and nitrogen types; (**a**) 2:1 NH_4^+ (white circle), 2:1 NO_3^- (white
430 diamond), 2:1 urea (white triangle), (**b**) 12:1 NH_4^+ (black circle) 12:1 NO_3^- (black diamond), 12:1 urea
431 (black triangle). The sorption conditions were; pH = 4.5, contact time = 24 h, biosorbent dose = 1 g L^{-1},
432 agitation = 100 rpm, initial metal concentration (C0) = 0.016-2.77 mmol L^{-1}, temperature = 24°C,
433 light = constant with 30-40 µmol photons m^{-2} s^{-1} (*n* = 1-3, *error bars* = 1 SD).

434

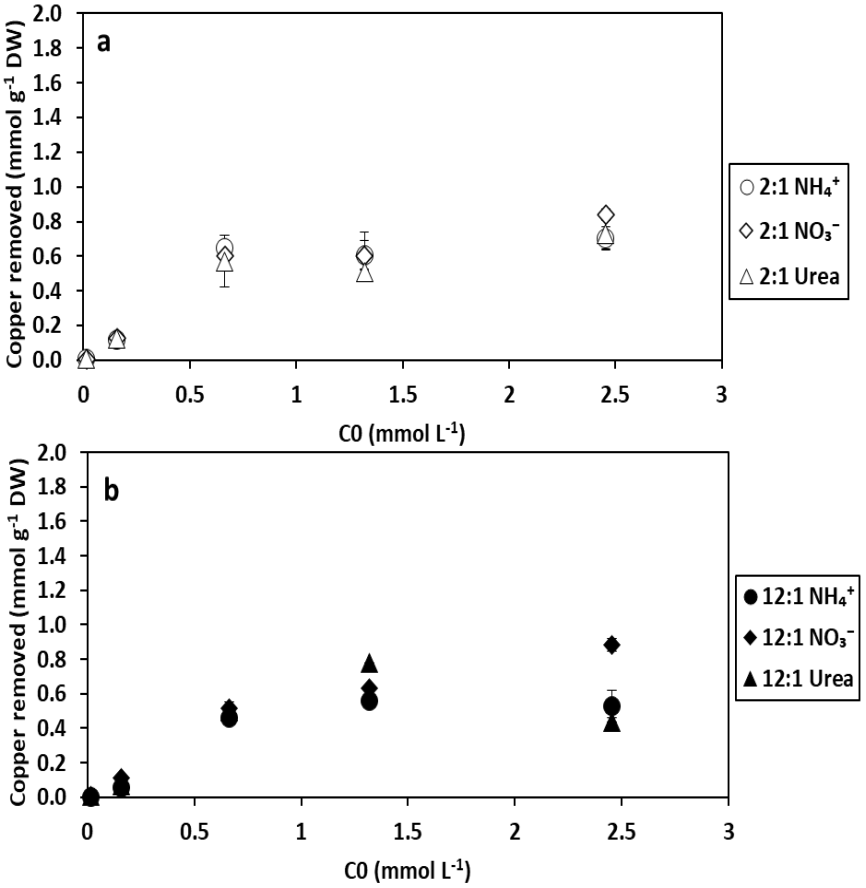

435

436 **Figure 4.** Copper removal per unit dry weight (DW) by *Cladophora parriaudii* biomass previously
437 cultivated under different N:P ratios and nitrogen types; (**a**) 2:1 NH_4^+ (white circle), 2:1 NO_3^- (white
438 diamond), 2:1 urea (white triangle), (**b**) 12:1 NH_4^+ (black circle) 12:1 NO_3^- (black diamond), 12:1 urea
439 (black triangle). The sorption conditions were; pH = 4.5, contact time = 24 h, biosorbent dose = 1 g L^{-1},
440 agitation = 100 rpm, initial metal concentration (C0) = 0.015-2.45 mmol L^{-1}, temperature = 24°C,
441 light = constant with 30-40 µmol photons m^{-2} s^{-1} (*n* = 1-3, *error bars* = 1 SD).

442

443 *3.3.* FT-IR Spectra of *C. parriaudii*

444 The absorbance spectra of the *C. parriaudii* biomass pre- and post- metal exposure was obtained for
445 all nutrient regimes. However, since the spectra appeared very similar between treatments, only
446 data relating to a 2:1 NO_3^- regime is presented here as an exemplar (Fig. 5). The FT-IR spectra for all
447 other regimes can be found in the Supporting Information.

448 The spectra from biomass without exposure to metals had a similar distribution of peaks, peak
449 shape, and wavenumber, regardless of cultivation regime. The spectra presented here (Fig. 5) are
450 very similar to those obtained from *Cladophora glomerata* biomass (Michalak et al., 2018) or from a
451 variety of cellulosic powders from *C. glomerata* (Suciyati et al., 2021). There were strong bands
452 present in the range of 3400-2800 cm^{-1}, which can be attributed to functional groups present in
453 proteins, lipids, carbohydrates and cellulose. There were intense peaks at 1650-1630 cm^{-1} and 1550-
454 1530 cm^{-1} caused by amine groups I and II, respectively. There were a variety of peaks in the range of
455 1460-1310 cm^{-1} that can be assigned to functional groups arising from cellulose, proteins, lipids, and
456 sulphur-containing components. There was a prominent peak at 1250-1210 cm^{-1} attributed to amine
457 group III and phosphodiester bonding of phospholipids. The remaining peaks at this lower end of the
458 spectrum can mostly be assigned to mono- and poly-saccharides, cellulose, aliphatics of the cell wall
459 and aromatic compounds (Fig. 5). Coupling the differences in biochemical composition (Table 2) and
460 the comparability of FTIR-ATR spectra between treatments (Fig. 5 & Supplementary Information)
461 suggests that cultivation under different nutrient regimes yields biomass of varying composition;
462 however, this does not necessarily translate into the synthesis of different molecules between
463 different nutrient regimes, but more likely in the quantity or proportion of molecules or functional
464 groups being different. This has been demonstrated in studies that have measured the IR spectra of
465 micro-organisms temporally and, therefore, of varying biochemical composition (Ami et al., 2014;
466 Dean et al., 2010). Unfortunately, this cannot be verified within this study using the employed FTIR-
467 ATR method since the algal biomass sample preparations were non-homogenous and, as such, they
468 did not meet the implicit requirements for Beer's Law (Griffiths, 2006): the FTIR-ATR analysis should
469 hence be considered as qualitative only, rather than quantitative. Therefore, comparison between
470 spectra is limited to the presence/absence of bands, shifts in wavenumber, or the relative peak size
471 within an individual spectrum.

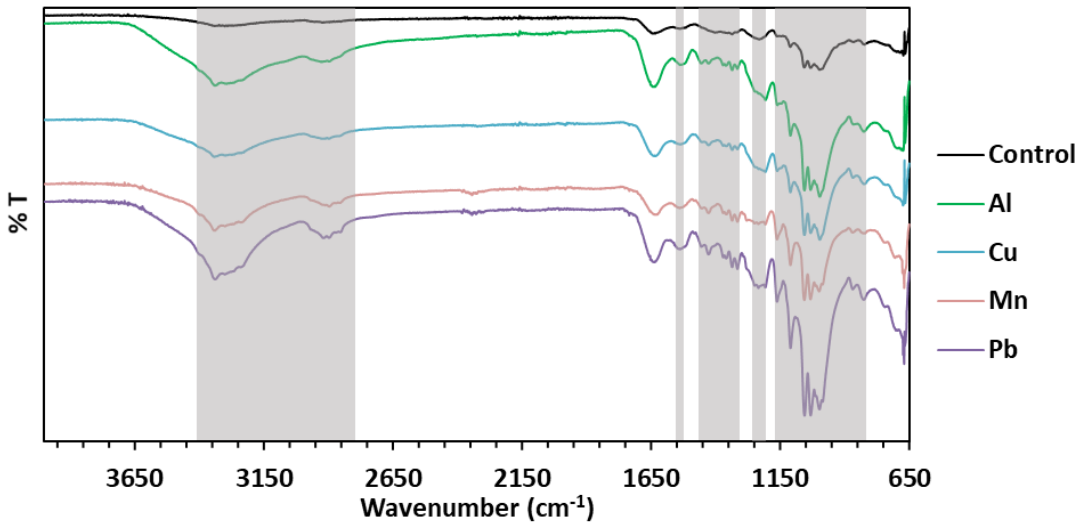

Figure 5. The Infrared spectra of *C. parriaudii* biomass after cultivation under a 2:1 NO_3^- regime obtained before (black) and after metal adsorption with aluminium (green), copper (blue), manganese (pink), and lead (purple). Each line is an average of 25 scans, baseline corrected and atmospheric CO_2/H_2O removed. To prevent overlap between spectra and to ease visualisation, a constant correction factor has been applied to the % transmission (% T). The main wavenumber ranges involved in metal adsorption across treatments have been highlighted in grey.

After metal sorption, the IR spectra were obtained from the metal loaded biomass (Fig. 5 and Supporting Info). Although the spectra from metal loaded biomass appeared near identical to those without any metal exposure, there are some subtle, yet consistent, differences between them. This indicates that certain functional groups were always involved in metal sorption. For instance, after exposure to all metals tested, the intense peak at amine III and phosphodiester peak 1250-1210 cm^{-1} changed shape, suggesting that the phospholipid membrane is involved in metal sorption. The amine peak at 1409-1403 cm^{-1}, visible in metal-free biomass, was not present in all metal loaded biomass: instead, there was the emergence of six smaller peaks within the same region. In addition, an increase in relative intensity was observed between 3347-3334 cm^{-1}, which can be attributed to symmetric stretching of N-H and O-H bonds within amide group A, water, and polysaccharides including cellulose (Duygu et al., 2012; Suciyati et al., 2021). There were frequent, yet inconsistent, changes in peak shape or wavenumber in the regions of 3405-3390 cm^{-1} which is assigned to stretching of -OH groups of water; 2920-2850 cm^{-1} caused by stretching of CH, CH_2 and CH_3 groups

present in fatty acids and polysaccharides; 1650-1630 cm^{-1} assigned to functional groups relating to amide group I and the relative intensity of the peaks at 1160 cm^{-1} and 1056-990 cm^{-1}, which were assigned to cellulose and polysaccharides, respectively. Since these changes in the FTIR-ATR spectra are inconsistent between treatments, they are likely to be indicative of the differences in relationships between the metal removal and biochemical data discussed earlier. Similar results were recorded by (Michalak et al., 2018) with *Cladophora*, where carboxyl and hydroxy groups in the regions of 1500-1400 and 1280-1200 cm^{-1} were effective for the removal of Mg, Mn, and Cr ions.

Following copper biosorption, there was a strong reduction in relative peak intensities with functional groups associated with carbohydrates (*e.g.* 1056 and 1033 cm^{-1}) when the biomass was cultivated under a 2:1 N:P regime or with a 12:1 NO_3^- as the nitrogen source. These nutrient regimes yielded biomass with elevated carbohydrate content (37.5-44.2% DW versus 32-34% DW) (Table 2) and was coincident with greater metal removal (0.704-0.885 mmol g^{-1} DW versus 0.435-0.53 mmol g^{-1} DW) (Fig. 3). This suggests that copper has a stronger affinity for functional groups present in polysaccharides and that carbohydrate rich biomass is suitable for its removal.

Similarly, the biomass with the greatest Mn removal was propagated under either 2:1 NH_4^+ or 12:1 urea regime (Fig. 4). This biomass was characterised by having either a high proportion of carbohydrates or protein, and consequently there was evident reduction in peak intensities at 1637, 1056, 1033, and 998 cm^{-1} that are assigned to functional groups associated with these macromolecules. All of these functional groups that are involved in metal biosorption are assigned to carbohydrates, proteins, and other macromolecules that may be located in or around the cell wall and membrane. A similar result has been found in the literature where there was a significant increase in removal capacity of chitinous material when associated proteins were also present with amine and carboxylic functional groups principally involved in sorption (Robinson-Lora and Brennan, 2010).

3.4. SEM Analysis

In order to understand if metal biosorption was influenced by the surface of the cell, or if metal bonding was localised to specific sites, SEM-BSE micrographs were taken of the *C. parriaudii* biomass after metal exposure (Fig. 6). Since all micrographs appeared similar visually, the micrograph depicting biomass cultivated with a 2:1 NO_3^- regime is used as an exemplar, with all other micrographs available in the Supporting Information. There was no apparent difference in the cellular structure between nutritional treatments with all filaments being nonporous, yet appearing furrowed or grooved, which was assumed to be due to the lyophilisation procedure prior to metal exposure. This indicates that neither the nutrient regime, nor metal type influenced the gross cellular morphology or surface topography of the cell. In addition, the SEM-BSE micrographs revealed that there were bright *clusters* present on the cell surface (Fig. 6), with EDX analysis indicating that heavy metals were present within these clusters (Fig. 7). Furthermore, these clusters were of irregular size and shape and occurred randomly across the filament surface and not confined to specific locations (*e.g.* furrows or damaged areas). These micrographs suggest that nutrient regime has little to no impact upon cell surface topography, which in turn has a minimal influence on metal biosorption.

The elemental spectra of different surface locations of each sample was determined by EDX (Fig. 7). Specifically, in order to avoid any potential inter-sample variation in biochemical composition, spectra were obtained from areas of the cell surface where metals were thought to be less prevalent (*i.e.*, without clear visual evidence of clusters) (Fig. 7a, c, e, and g). All samples from these cell localities contained elements expected within algal biomass, including a high proportion of oxygen and sulphur, as well as phosphorus. Light and alkaline metals such as sodium, magnesium, and calcium were also present, which are elements required for the normal functioning of the algal cell. Similar elements were also found in native *Cladophora* biomass analysed by EDX analysis (Amro and Abhary, 2019). Unfortunately, the study by (Amro and Abhary, 2019) did not reanalyse the EDX

543 spectra after the biomass was used for the sorption of lead and cadmium ions, meaning that
544 potential mechanisms of metal removal may have been overlooked. In this study, the target heavy
545 metals were detected upon all areas of the biomass following sorption, albeit to a relatively low
546 degree, which suggests that the whole surface of the biomass was involved in metal sorption.
547 However, EDX spectra was measured at locations of the cell where the clusters were present (Fig.
548 7b, d, f, and h). Signals for the target heavy metals used in this study were generally greater in these
549 areas, hence indicating that these metals were predominantly present within these clusters. In the
550 vast majority of instances, the spectra from the clusters (Fig. 7b, d, f, and h) contained stronger
551 signals for O, P, Fe compared to other areas of the cell. The clusters also frequently contained
552 stronger signals of Mg, Ca, and Si, suggesting a variety of mechanisms for metal sorption including
553 ion exchange, complexation and micro-precipitation (Gadd, 2009; Mehta and Gaur, 2005). These
554 elements all serve key functions within the cell. For instance, Mg is the core ion in chlorophylls
555 located in membrane-bound chloroplasts in close proximity to the cell surface (Brock, 1973). Iron
556 has numerous functions within the cell, including nitrogen assimilation via ferrodoxin (Raven et al.,
557 1999), whereas, P is a key constituent of the phospholipid bilayer of cell membranes (Ami et al.,
558 2014), which FTIR analysis (Fig. 5) indicated that the component phosphodiester bonds, at 1250-
559 1210 cm^{-1}, play a role in biosorption. Studies have improved the ion exchange capacity of biosorbent
560 material by pre-treating it with calcium (Davis et al., 2003), explaining why metals have a preference
561 for areas with strong Ca. Silicon, on the other hand, is thought to have a healing or protective role in
562 sporophytes of *Saccharina japonica* (Mizuta and Yasui, 2012). Si also has stress alleviation roles in
563 higher plants by complexing, co-precipitating, or compartmentalising (toxic) metals or via
564 stimulation of antioxidant systems (Liang et al., 2007). It was also noted that there was often a
565 reduction in the relative proportion of S within the clusters. This was especially true after exposure
566 to copper. The cell wall of *Cladophora* contains sulphated polysaccharides (Arata et al., 2017), and
567 given that carbohydrate rich biomass was the most effective for the removal of copper (Table 2 &
568 Fig. 3), it is likely that cell wall associated sulphated polysaccharides were involved in copper

sorption. These elements with varying signal after sorption, identified by EDX analysis, are pivotal for photosynthesis, protein synthesis, and cellular structure. All occur in or around the cell surface and are influenced by age, nutrient regime, cultivation conditions, and seasonality (Kumar and Sahoo, 2017; Schiener et al., 2015), which could have significant implications when utilising material collected from the field. For instance, (Kumar and Sahoo, 2017) showed age and seasonal related variability in the Ca, Mg, and Fe (among others) content of *Sargassum wightii* biomass.

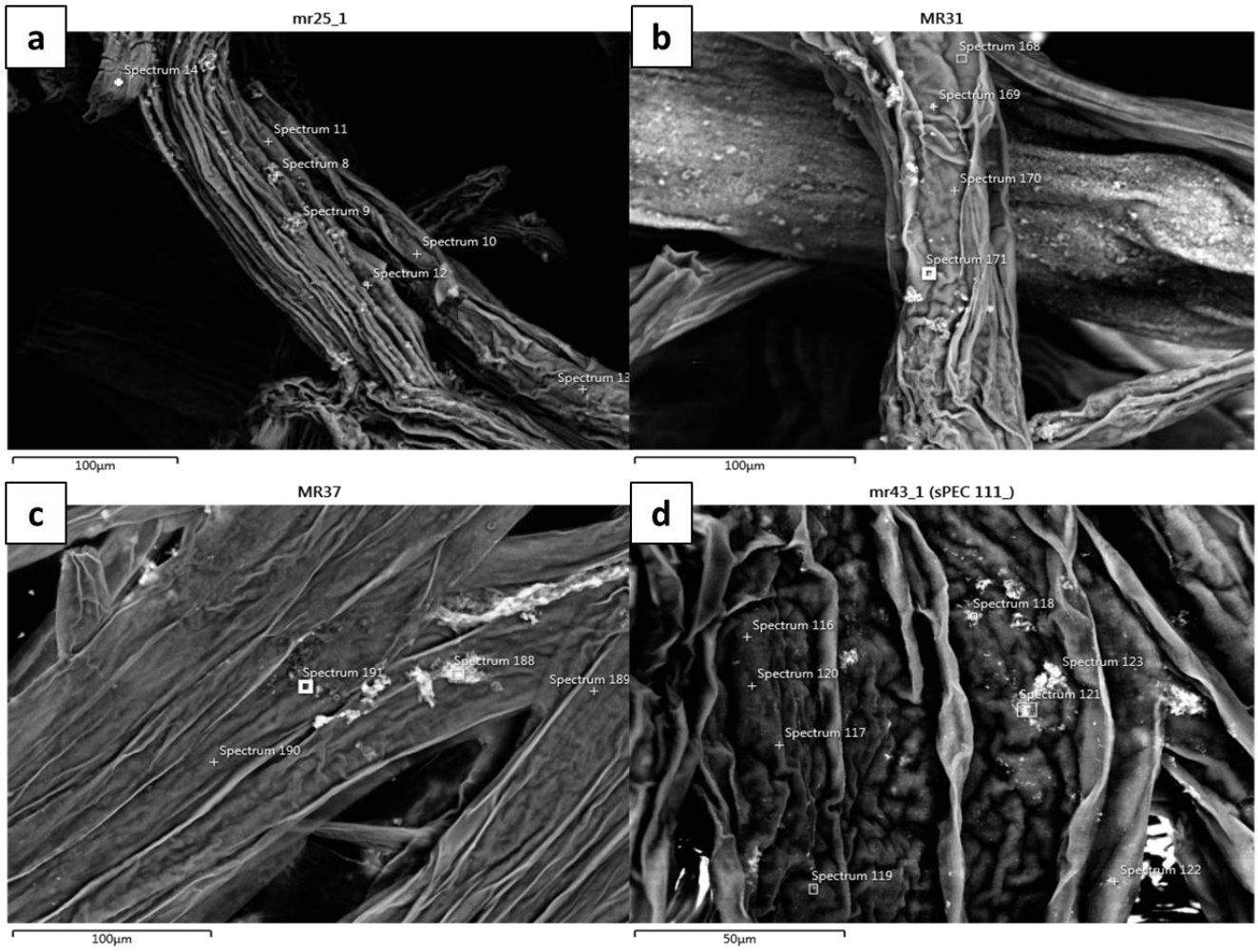

Figure 6. The cell surface of *Cladophora parriaudii*, previously cultivated under a 2:1 NO_3^- medium, after exposure to a) Al, b) Cu, c) Mn, d) Pb. Images were attained with Scanning Electron Microscopy using the back-scattered electrons (BSE) technique at 20 kV and ~1.2-1.5 K x magnification. This

figure depicts the similarity in surface structure, regardless of the nutrient regime. Note the presence of bright irregularly shaped *clusters* scattered randomly across the surfaces of all of the filaments.

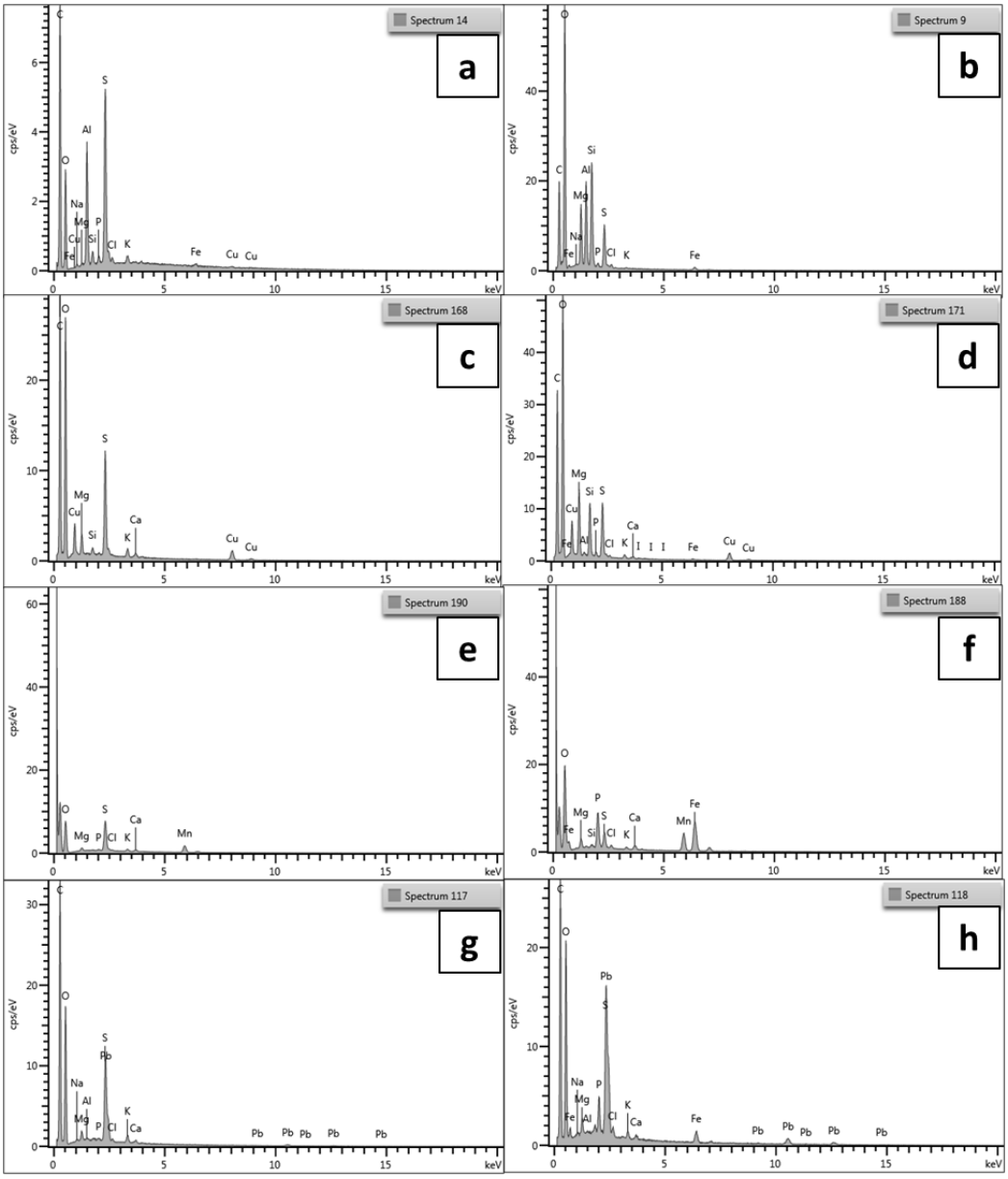

Figure 7. The Scanning Electron Microscopy – Energy Dispersive X-Ray elemental spectra of *Cladophora parriaudii*, previously cultivated under a 2:1 NO_3^- nutrient regime and after exposure to metals: Al (a & b), Cu (c & d), Mn (e & f), Pb (g & h). The spectra on the left-hand side (a, c, e, and g) were obtained from areas on the cell surface which were deemed "pristine", or as having no visual evidence of metal/contaminant bonding. Spectra on the right-hand side (b, d, f, and h) were obtained from areas on the cell surface in which metal was present, typically as a bright "cluster". The specific locations of each spectrum are denoted in the corresponding images in Fig. 1. Please note differences in the y-axes.

By taking a holistic overview of this research and combining the clustering behaviour of metals from the SEM-BSE micrographs (Fig. 6), their FTIR-ATR and EDX spectra (Fig. 7), the biochemical composition of the biomass (Table 2), the roles of each element within the cell and a review of the literature, there are multiple mechanisms involved in adsorption, which is a very complex process. However, this complexity offers a variety of avenues of further research which lead on from this study. These include the development of a quantifiable method for the FTIR analysis, as correlating this empirically with biochemical and metal sorption values would be beneficial (Mayers et al., 2014). Investigating the impact of different nutrient regimes upon the optimised metal removal parameters (e.g. pH, temperature), in addition to the influence of counter ions within the metallic salts provided (e.g. chloride or sulphate)(Michalak et al., 2018), would also be important to assess the maximum adsorption capacity of the biomass. It would also be interesting to investigate the effects of C:N ratio during cultivation to determine if this has any resultant and beneficial impact upon biomass production in terms of yield and of extracellular polymeric substances (EPS), which would play a role in metal sorption (Gupta and Diwan, 2017; Sepehri et al., 2020). Similarly, the impacts upon different nutrient regimes upon living material biomass production, used for simultaneous metal removal, to assess if these can enhance toxicity or lead to detoxification and enhanced viability and biomass production. Greater understanding of the mechanisms involved with sorption and better description of the biosorbent material by adopting better fitting mathematical mass transfer models (Fulazzaky, 2011), or by determining the selectivity of functional groups (e.g. Boehm titration, inverse gas chromatography (IGC) (Fulazzaky et al., 2019). Finally, investigations into enhancing the circularity and economic and environmental sustainability of biosorption in practice via life cycle assessments (LCA), desorption, prior extraction of high-value compounds, or potential uses of the spent biosorbent material e.g. soil amendment (Pap et al., 2020).

4. Conclusions

The main purpose of this study was to demonstrate that the pre-processing or production of algal biomass could have important implications upon the resultant biochemical and pollutant removal qualities of a biosorbent material. As such, the *C. parriaudii* biomass employed within this study was produced by cultivating with different nutrient regimes, designed to elicit varying biochemical profiles. Both the nitrogen type and the N:P ratio had an impact upon the final composition of the biomass, particularly in terms of the protein and carbohydrate content, which ranged from 8.5-13.6% and 32-44.2% DW, respectively. The material was then used for the adsorption of different metals, namely Al, Cu, Mn, and Pb, provided across a concentration range. Metal removal varied with metal type, initial concentration, and the nutrient regime in which the biomass produced with values of 0.023-1.636, 0.005-0.885, 0.005-0.658, and 0.002-0.855 mmol g^{-1} DW recorded for Al, Cu, Mn, and Pb, respectively. FTIR analysis indicated that functional groups associated with proteins and polysaccharides play an important role in metal adsorption, while SEM-EDX indicated that elements including Ca, Fe, Mg, P, and Si are involved with adsorption. Since all other experimental factors were identical, the observed variation and means of metal removal between treatments (Figs 1-4 & Supplementary Table S1) can only be attributed to biological variability and cell surface properties induced by the cultivation under different types of media. Therefore, through a broad and robust methodology, the experimental hypotheses set out in this study have been proven: nutritional history, and putatively other biological aspects as an indirect extension of this, play a significant role in the biomass qualities produced and their subsequent usefulness for pollutant removal. Previously published studies of a similar nature will have overlooked this aspect making scientific reproducibility a challenge. Furthermore, this could explain the broad variation in metal removal values on an inter- and intra-species level previously reported. Since cultivation conditions have a considerable influence upon metal removal, much greater consideration should be granted to the conditions used to produce biosorbent material in future studies of this kind. Finally, understanding

644 the influence of biomass cultivation processes could have significant practical applications in terms
645 of reproducibility, pollutant removal efficacy and consistency, and the cost of biosorbent materials
646 produced.

647

648 Supporting Information

649 Figures and Tables relating to FTIR-ATR, SEM-BSE and EDX spectra are available.

650

651 Acknowledgments

652 The authors acknowledge the joint funding of an E3 Doctoral Training Partnership from NERC and
653 EPSCR. The authors also thank staff from the University of Edinburgh: Dr. Nicola J. Cayzer from the
654 School of Geosciences for the SEM analysis and guidance with the results and manuscript; Dr. Lorna
655 Eades from the School of Chemistry for ICP-OES analysis; and Dr. Mike Davidson from the Institute
656 for Materials and Processes, School of Engineering, for use of the FTIR. The authors are grateful to
657 Prof. Mikhail Zubkov and Dr. Lucie Novoveská, both from SAMS, for their recommendations and
658 insightful comments on the manuscript. The authors are grateful to the anonymous reviewers of the
659 Journal of Environmental Management for their suggestions and comments which have improved
660 the quality and clarity of this work.

661

662 Author Information

663 M.E.R. and A.J.C.S. conceived and planned the project. M.E.R. conducted the experiments,
664 generated, collated, and processed the data. M.E.R. and A.J.C.S. interpreted the results. M.E.R.
665 wrote the manuscript. M.E.R., M.S.S., J.G.D., and A.J.C.S. reviewed and edited the manuscript.
666 M.S.S., J.G.D., and A.J.C.S. supervised the project and acquired the funding.

Author Information

The authors declare that they have no competing interests.

References

Ali, H., Khan, E., Sajad, M.A., 2013. Phytoremediation of heavy metals—concepts and applications. Chemosphere 91, 869–881.

Ami, D., Posteri, R., Mereghetti, P., Porro, D., Doglia, S.M., Branduardi, P., 2014. Fourier transform infrared spectroscopy as a method to study lipid accumulation in oleaginous yeasts. Biotechnol. Biofuels 7, 1–14.

Amro, A.N., Abhary, M.K., 2019. Removal of lead and cadmium ions from water using *Cladophora* biomass. Pol. J. Environ. Stud. 28, 1–8.

Arata, P.X., Alberghina, J., Confalonieri, V., Errea, M.I., Estevez, J.M., Ciancia, M., 2017. Sulfated polysaccharides in the freshwater green macroalga *Cladophora surera* not linked to salinity adaptation. Front. Plant Sci. 8, 1927.

Arumugam, N., Chelliapan, S., Thirugnana, S.T., Jasni, A.B., 2020. Optimisation of heavy metals uptake from leachate using red seaweed *Gracilaria changii*. J. Environ. Treat. Tech. 8, 1089–1092.

Blaby-Haas, C.E., Merchant, S.S., 2012. The ins and outs of algal metal transport. BBA-Mol. Cell Res. 1823, 1531–1552.

Brock, T.D., 1973. Lower pH limit for the existence of blue-green algae: evolutionary and ecological implications. Science 179, 480–483.

Calderón, O.A.R., Abdeldayem, O.M., Pugazhendhi, A., Rene, E.R., 2020. Current updates and perspectives of biosorption technology: an alternative for the removal of heavy metals from wastewater. Current Pollution Reports 6, 8–27.

Camacho, D.H., Gerongay, S.R.C., Macalinao, J.P.C., 2013. *Cladophora* cellulose-polyaniline composite for remediation of toxic chromium (VI). Cell. Chem. Technol. 47, 125–132.

Chojnacka, K., Chojnacki, A., Górecka, H., 2004. Trace element removal by *Spirulina* sp. from copper smelter and refinery effluents. Hydrometallurgy 73, 147–153.

Chopin, T., Gallant, T., Davison, I., 1995. Phosphorus and nitrogen nutrition in *Chondrus crispus* (Rhodophyta): Effects on total phosphorus and nitrogen content, carrageenan production, and photosynthetic pigments and metabolism 1. J. Phycol. 31, 283–293.

Darmovzalova, J., Boghi, A., Otten, W., Eades, L.J., Roose, T., Kirk, G.J.D., 2020. Uranium diffusion and time-dependent adsorption–desorption in soil: A model and experimental testing of the model. European Journal of Soil Science 71, 215–225.

Davis, T.A., Volesky, B., Mucci, A., 2003. A review of the biochemistry of heavy metal biosorption by brown algae. Water Res. 37, 4311–4330.

Davis, T.A., Volesky, B., Vieira, R., 2000. *Sargassum* seaweed as biosorbent for heavy metals. Water Res. 34, 4270–4278.

Dean, A.P., Sigee, D.C., Estrada, B., Pittman, J.K., 2010. Using FTIR spectroscopy for rapid determination of lipid accumulation in response to nitrogen limitation in freshwater microalgae. Bioresource Technol. 101, 4499–4507.

Deng, L., Su, Y., Su, H., Wang, X., Zhu, X., 2007. Sorption and desorption of lead (II) from wastewater by green algae *Cladophora fascicularis*. J. Hazard. Mater. 143, 220–225.

Deng, L., Su, Y., Su, H., Wang, X., Zhu, X., 2006. Biosorption of copper (II) and lead (II) from aqueous solutions by nonliving green algae *Cladophora fascicularis*: equilibrium, kinetics and environmental effects. Adsorption 12, 267–277.

Dubois, M., Gilles, K.A., Hamilton, J.K., Rebers, P.A. t, Smith, F., 1956. Colorimetric method for determination of sugars and related substances. Analytical chemistry 28, 350–356.

Duygu, D.Y., Udoh, A.U., Ozer, T.B., Akbulut, A., Erkaya, I.A., Yildiz, K., Guler, D., 2012. Fourier transform infrared (FTIR) spectroscopy for identification of *Chlorella vulgaris* Beijerinck 1890 and *Scenedesmus obliquus* (Turpin) Kützing 1833. African Journal of Biotechnology 11, 3817–3824.

El-Naggar, N.E.-A., Rabei, N.H., 2020. Bioprocessing optimization for efficient simultaneous removal of methylene blue and nickel by *Gracilaria* seaweed biomass. Scientific Reports 10, 1–21.

Fawzy, M.A., 2020. Biosorption of copper ions from aqueous solution by *Codium vermilara*: Optimization, kinetic, isotherm and thermodynamic studies. Adv. Powder Technol. 31, 3724–3735.

Figueira, P., Henriques, B., Teixeira, A., Lopes, C.B., Reis, A.T., Monteiro, R.J.R., Duarte, A.C., Pardal, M.A., Pereira, E., 2016. Comparative study on metal biosorption by two macroalgae in saline waters: single and ternary systems. Environ. Sci. Pollut. Res. 23, 11985–11997.

Förstner, U., Wittmann, G.T.W., 1981. Metal pollution in the aquatic environment. Springer Berlin Heidelberg, Berlin, Germany.

740 Fournier, E., 2001. Colorimetric Quantification of Carbohydrates, in: Wrolstad, R.
741 (Ed.), Current Protocols in Food Analytical Chemistry. John WIley and Sons,
742 Hoboken, NJ, USA.

743 Freundlich, H., 1907. Über die adsorption in lösungen. Zeitschrift für physikalische
744 Chemie 57, 385–470.

745 Fu, F., Wang, Q., 2011. Removal of heavy metal ions from wastewaters: a review. J.
746 Environ. Manage. 92, 407–418.

747 Fulazzaky, M.A., 2011. Determining the resistance of mass transfer for adsorption of
748 the surfactants onto granular activated carbons from hydrodynamic column.
749 Chem. Eng. J. 166, 832–840.

750 Fulazzaky, M.A., Abdullah, S., Salim, M.R., 2015. Fundamentals of mass transfer and
751 kinetics for biosorption of oil and grease from agro-food industrial effluent by
752 Serratia marcescens SA30. RSC Adv. 5, 104666–104673.

753 Fulazzaky, M.A., Nuid, M., Aris, A., Fulazzaky, M., Sumeru, K., Muda, K., 2019. Mass
754 transfer kinetics of phosphorus biosorption by aerobic granules. Journal of
755 Water Process Engineering 31, 100889.

756 Gadd, G.M., 2009. Biosorption: critical review of scientific rationale, environmental
757 importance and significance for pollution treatment. J. Chem. Technol. Biot. 84,
758 13–28.

759 Gadd, G.M., 2000. Bioremedial potential of microbial mechanisms of metal
760 mobilization and immobilization. Curr. Opin. Biotech. 11, 271–279.

761 Griffiths, M.J., Garcin, C., van Hille, R.P., Harrison, S.T.L., 2011. Interference by
762 pigment in the estimation of microalgal biomass concentration by optical
763 density. J. Microbiol. Meth. 85, 119–123.

764 Griffiths, P.R., 2006. Beer's Law, in: Griffiths, P.R. (Ed.), Handbook of Vibrational
765 Spectroscopy. John Wiley & Sons, Ltd, Chichester, UK.

766 Guillard, R.R.L., Ryther, J.H., 1962. Studies of marine planktonic diatoms: I. *Cyclotella*
767 *nana* Hustedt, and *Detonula confervacea* (Cleve) Gran. Can. J. Microbiol. 8,
768 229–239.

769 Gupta, P., Diwan, B., 2017. Bacterial exopolysaccharide mediated heavy metal
770 removal: a review on biosynthesis, mechanism and remediation strategies.
771 Biotechnology Reports 13, 58–71.

772 He, J., Chen, J.P., 2014. A comprehensive review on biosorption of heavy metals by
773 algal biomass: materials, performances, chemistry, and modeling simulation
774 tools. Bioresource Technol. 160, 67–78.

775 Henriques, B., Rocha, L.S., Lopes, C.B., Figueira, P., Duarte, A.C., Vale, C., Pardal,
776 M.A., Pereira, E., 2017. A macroalgae-based biotechnology for water
777 remediation: Simultaneous removal of Cd, Pb and Hg by living *Ulva lactuca*. J.
778 Environ. Manage. 191, 275–289.

779 Henriques, C.A., da Costa, A.C.A., dos Reis, M.M., Costa, A.L.H., Luna, A.S., 2011.
780 Batch and fixed-bed column biosorption of manganese ion by *Sargassum*
781 *filipendula*. Electron. J. Biotechn. 14, 8.

782 Holan, Z.R., Volesky, B., 1994. Biosorption of lead and nickel by biomass of marine
783 algae. Biotechnol. Bioeng. 43, 1001–1009.

784 Islam, M.S., Ahmed, M.K., Raknuzzaman, M., Habibullah-Al-Mamun, M., Islam, M.K.,
785 2015. Heavy metal pollution in surface water and sediment: a preliminary
786 assessment of an urban river in a developing country. Ecol. Indic. 48, 282–291.

787 Kar, D., Sur, P., Mandai, S.K., Saha, T., Kole, R.K., 2008. Assessment of heavy metal
788 pollution in surface water. Int. J. Environ. Sci. Te. 5, 119–124.

789 Kotrba, P., 2011. Microbial biosorption of metals—general introduction, in:
790 Microbial Biosorption of Metals. Springer, pp. 1–6.

791 Kumar, S., Sahoo, D., 2017. A comprehensive analysis of alginate content and
792 biochemical composition of leftover pulp from brown seaweed *Sargassum*
793 *wightii*. Algal Res. 23, 233–239.

794 Langmuir, I., 1918. The adsorption of gases on plane surfaces of glass, mica and
795 platinum. J. Am. Chem. Soc. 40, 1361–1403.

796 Lee, H.S., Suh, J.H., Kim, I.B., Yoon, T., 2004. Effect of aluminum in two-metal
797 biosorption by an algal biosorbent. Miner. Eng. 17, 487–493.

798 Lee, Y.-C., Chang, S.-P., 2011. The biosorption of heavy metals from aqueous solution
799 by *Spirogyra* and *Cladophora* filamentous macroalgae. Bioresource Technol.
800 102, 5297–5304.

801 Liang, Y., Sun, W., Zhu, Y.-G., Christie, P., 2007. Mechanisms of silicon-mediated
802 alleviation of abiotic stresses in higher plants: a review. Environ. Pollut. 147,
803 422–428.

804 Mack, C., Wilhelmi, B., Duncan, J.R., Burgess, J.E., 2007. Biosorption of precious
805 metals. Biotechnol. Adv. 25, 264–271.

806 Manning, D.A.C., Baptista, J., Limon, M.S., Brandt, K., 2017. Testing the ability of
807 plants to access potassium from framework silicate minerals. Sci. Total Environ.
808 574, 476–481.

809 Mayers, J.J., Flynn, K.J., Shields, R.J., 2014. Influence of the N: P supply ratio on
810 biomass productivity and time-resolved changes in elemental and bulk
811 biochemical composition of *Nannochloropsis* sp. Bioresource Technol. 169,
812 588–595.

813 Mehta, S.K., Gaur, J.P., 2005. Use of algae for removing heavy metal ions from
814 wastewater: progress and prospects. Crit. Rev. Biotechnol. 25, 113–152.

815 Michalak, I., Mironiuk, M., Marycz, K., 2018. A comprehensive analysis of
816 biosorption of metal ions by macroalgae using ICP-OES, SEM-EDX and FTIR
817 techniques. PloS one 13, e0205590.

Mizuta, H., Yasui, H., 2012. Protective function of silicon deposition in *Saccharina japonica* sporophytes (Phaeophyceae). J. Appl. Phycol. 24, 1177–1182.

Navarrete, A., González, A., Gómez, M., Contreras, R.A., Díaz, P., Lobos, G., Brown, M.T., Sáez, C.A., Moenne, A., 2019. Copper excess detoxification is mediated by a coordinated and complementary induction of glutathione, phytochelatins and metallothioneins in the green seaweed *Ulva compressa*. Plant Physiol. Bioch. 135, 423–431.

Özer, A., Özer, D., Ekİz, H.İ., 2004. The equilibrium and kinetic modelling of the biosorption of copper (II) ions on *Cladophora crispata*. Adsorption 4, 317–326.

Pap, S., Kirk, C., Bremner, B., Sekulic, M.T., Shearer, L., Gibb, S.W., Taggart, M.A., 2020. Low-cost chitosan-calcite adsorbent development for potential phosphate removal and recovery from wastewater effluent. Water Res. 173, 115573.

Pavasant, P., Apiratikul, R., Sungkhum, V., Suthiparinyanont, P., Wattanachira, S., Marhaba, T.F., 2006. Biosorption of Cu^{2+}, Cd^{2+}, Pb^{2+}, and Zn^{2+} using dried marine green macroalga *Caulerpa lentillifera*. Bioresource Technol. 97, 2321–2329.

Prasher, S.O., Beaugeard, M., Hawari, J., Bera, P., Patel, R.M., Kim, S.H., 2004. Biosorption of heavy metals by red algae (*Palmaria palmata*). Environ. Technol. 25, 1097–1106.

Raven, J.A., Evans, M.C.W., Korb, R.E., 1999. The role of trace metals in photosynthetic electron transport in O2-evolving organisms. Photosynth. Res. 60, 111–150.

Reza, R., Singh, G., 2010. Heavy metal contamination and its indexing approach for river water. Int. J. Environ. Sci.Te. 7, 785–792.

Robinson-Lora, M.A., Brennan, R.A., 2010. Biosorption of manganese onto chitin and associated proteins during the treatment of mine impacted water. Chem. Eng. J. 162, 565–572.

Romera, E., González, F., Ballester, A., Blázquez, M.L., Munoz, J.A., 2007. Comparative study of biosorption of heavy metals using different types of algae. Bioresource Technol. 98, 3344–3353.

Ross, M.E., Davis, K., McColl, R., Stanley, M.S., Day, J.G., Semião, A.J.C., 2018. Nitrogen uptake by the macro-algae *Cladophora coelothrix* and *Cladophora parriaudii*: Influence on growth, nitrogen preference and biochemical composition. Algal Res. 30, 1–10.

Ross, M.E., Stanley, M.S., Day, J.G., Semião, A.J.C., 2017. A comparison of methods for the non-destructive fresh weight determination of filamentous algae for growth rate analysis and dry weight estimation. J. Appl. Phycol. 29, 2925–2936.

Sari, A., Tuzen, M., 2009. Equilibrium, thermodynamic and kinetic studies on aluminum biosorption from aqueous solution by brown algae (*Padina pavonica*) biomass. J. Hazard. Mater. 171, 973–979.

Sauer, K., 1980. A role for manganese in oxygen evolution in photosynthesis. Accounts Chem. Res. 13, 249–256.

Schiener, P., Black, K.D., Stanley, M.S., Green, D.H., 2015. The seasonal variation in the chemical composition of the kelp species *Laminaria digitata*, *Laminaria hyperborea*, *Saccharina latissima* and *Alaria esculenta*. J. Appl. Phycol. 27, 363–373.

Sepehri, A., Sarrafzadeh, M.-H., Avateffazeli, M., 2020. Interaction between *Chlorella vulgaris* and nitrifying-enriched activated sludge in the treatment of wastewater with low C/N ratio. J. Clean. Prod. 247, 119164.

Slocombe, S.P., Ross, M., Thomas, N., McNeill, S., Stanley, M.S., 2013. A rapid and general method for measurement of protein in micro-algal biomass. Bioresource Technol. 129, 51–57.

Sluiter, A., Hames, B., Ruiz, R., Scarlata, C., Sluiter, J., Templeton, D., Crocker, D., 2008. Determination of structural carbohydrates and lignin in biomass. Laboratory Analytical Procedure 1617, 1–16.

Suciyati, S.W., Manurung, P., Sembiring, S., Situmeang, R., 2021. Comparative study of *Cladophora* sp. cellulose by using FTIR and XRD, in: J. Phys.: Conf. Ser. IOP Publishing, p. 012075.

Tchounwou, P.B., Yedjou, C.G., Patlolla, A.K., Sutton, D.J., 2012. Heavy metal toxicity and the environment. Molecular, Clinical and Environmental Toxicology 133–164.

Tien, C.-J., 2002. Biosorption of metal ions by freshwater algae with different surface characteristics. Process Biochem. 38, 605–613.

Topal, M., Topal, E.I.A., Öbek, E., 2020. Remediation of pollutants with economical importance from mining waters: Usage of *Cladophora fracta*. Environmental Technology & Innovation 19, 100876.

Utomo, H.D., Tan, K.X.D., Choong, Z.Y.D., Yu, J.J., Ong, J.J., Lim, Z.B., 2016. Biosorption of heavy metal by algae biomass in surface water. Journal of Environmental Protection 7, 1547–1560.

Varol, M., Şen, B., 2012. Assessment of nutrient and heavy metal contamination in surface water and sediments of the upper Tigris River, Turkey. Catena 92, 1–10.

Vijayaraghavan, K., Joshi, U.M., 2014. Application of *Ulva* sp. biomass for single and binary biosorption of chromium (III) and manganese (II) ions: equilibrium modeling. Environ. Prog. Sust. 33, 147–153.

Volesky, B., Holan, Z.R., 1995. Biosorption of heavy metals. Biotechnol. Progr. 11, 235–250.

Wang, J., Chen, C., 2009. Biosorbents for heavy metals removal and their future. Biotechnol. Adv. 27, 195–226.

WHO, 2017. World Health Organization: Guidelines for drinking-water quality: Incorporating the first addendum, Fourth Edition. ed.

Zhang, H., Geng, G., Wang, J., Xin, Y., Zhang, Q., Cao, D., Ma, Y., 2019. The remediation potential and kinetics of cadmium in the green alga *Cladophora rupestris*. Environ. Sci. Pollut. Res. 26, 775–783.

Zhang, L., Yanjun, W.U., Xiaoyan, Q.U., Zhenshan, L., Jinren, N., 2009. Mechanism of combination membrane and electro-winning process on treatment and remediation of Cu^{2+} polluted water body. J. Environ. Sci. 21, 764–769.

Web References

https://www.ccap.ac.uk/our-cultures.htm

https://www.ccap.ac.uk/pdfrecipes.htm

926